DNAI2 Mutations Cause Primary Ciliary Dyskinesia with Defects in the Outer Dynein Arm

Niki Tomas Loges,[1,2] Heike Olbrich,[1] Lale Fenske,[1] Huda Mussaffi,[3] Judit Horvath,[4] Manfred Fliegauf,[1] Heiner Kuhl,[5] Gyorgy Baktai,[6] Erzsebet Peterffy,[6] Rahul Chodhari,[7] Eddie M.K. Chung,[7] Andrew Rutman,[8] Christopher O'Callaghan,[8] Hannah Blau,[3] Laszlo Tiszlavicz,[9] Katarzyna Voelkel,[10] Michal Witt,[10,11] Ewa Ziętkiewicz,[10] Juergen Neesen,[12] Richard Reinhardt,[5] Hannah M. Mitchison,[7] and Heymut Omran[1,*]

Primary ciliary dyskinesia (PCD) is a genetically heterogeneous disorder characterized by chronic destructive airway disease and randomization of left/right body asymmetry. Males often have reduced fertility due to impaired sperm tail function. The complex PCD phenotype results from dysfunction of cilia of the airways and the embryonic node and the structurally related motile sperm flagella. This is associated with underlying ultrastructural defects that frequently involve the outer dynein arm (ODA) complexes that generate cilia and flagella movement. Applying a positional and functional candidate-gene approach, we identified homozygous loss-of-function *DNAI2* mutations (IVS11+1G > A) in four individuals from a family with PCD and ODA defects. Further mutational screening of 105 unrelated PCD families detected two distinct homozygous mutations, including a nonsense (c.787C > T) and a splicing mutation (IVS3-3T > G) resulting in out-of-frame transcripts. Analysis of protein expression of the ODA intermediate chain DNAI2 showed sublocalization throughout respiratory cilia. Electron microscopy showed that mutant respiratory cells from these patients lacked DNAI2 protein expression and exhibited ODA defects. High-resolution immunofluorescence imaging demonstrated absence of the ODA heavy chains DNAH5 and DNAH9 from all *DNAI2* mutant ciliary axonemes. In addition, we demonstrated complete or distal absence of DNAI2 from ciliary axonemes in respiratory cells of patients with mutations in genes encoding the ODA chains DNAH5 and DNAI1, respectively. Thus, *DNAI2* and *DNAH5* mutations affect assembly of proximal and distal ODA complexes, whereas *DNAI1* mutations mainly disrupt assembly of proximal ODA complexes.

Introduction

Primary ciliary dyskinesia (PCD [MIM 242650]), also known as immotile cilia syndrome (ICS), is a rare, usually autosomal-recessive genetic disorder affecting cilia and flagella movement; it has an incidence of 1 in 20,000–30,000 people.[1] Motile cilia covering the epithelia of the upper and lower respiratory tract function to constantly move inhaled particles, cell debris, and microbes toward the throat.[2] Because PCD patients lack mucociliary clearance, recurrent infections of the upper and lower respiratory tract eventually cause permanent lung damage such as bronchiectasis in these patients.[3,4] Dysfunction of nodal cilia during early embryogenesis causes randomization of left/right body asymmetry, which explains why approximately half of affected PCD individuals have situs inversus.[5] The association of PCD and situs inversus is also referred to as Kartagener syndrome (KS [MIM 244400]). Interestingly, a subset of PCD patients have more severe laterality defects associated with complex heart defects.[6] Male PCD patients often have reduced fertility, which is explained by dysmotile sperm tails (flagella) that have an ultrastructure resembling that of respiratory cilia.

Cilia and flagella are hair-like structures extending from the cell surface.[7] Most motile cilia, such as respiratory cilia, have a 9 + 2 axoneme with an ultrastructure consisting of nine peripheral doublets surrounding two central tubules. The 9 + 2 configuration is also found in sperm flagella and has been preserved throughout evolution, but there are also motile cilia with a 9 + 0 configuration, e.g., nodal cilia. A number of multiprotein complexes, including radial spokes, nexin links, the central sheath, and dynein arms interconnect the different axonemal components. Outer dynein arms (ODAs) are connected to the peripheral microtubule A and generate motion by ATP-dependent reactions. The outer dynein arms are complex macromolecular assemblies containing different polypeptide chains classified according to their sizes as heavy (400–500 kDa), intermediate (45–110 kDa), and light chains (8–55 kDa), and these have been studied in detail in *Chlamydomonas reinhardtii*.[8] The dynein heavy chains form the globular heads and the stem of the ODA complexes and contain the ATPase and microtubule motor domains.

We recently showed that recessive mutations of *DNAH5* (MIM 603335) encoding an ODA heavy dynein chain are found in approximately 50% of PCD individuals with

[1]Department of Pediatrics and Adolescent Medicine, University Hospital Freiburg, Freiburg, Germany; [2]Faculty of Biology, Albert-Ludwigs-University, Freiburg, Germany; [3]Pulmonary Unit, Schneider Children's Medical Center of Israel, Petah-Tikva, Sackler School of Medicine, Tel-Aviv University, Tel-Aviv, Israel; [4]National Medical Center, Budapest, Hungaria; [5]Max-Planck Institute for Molecular Genetics, Berlin, Germany; [6]Pediatric Institute Svabhegy, Budapest, Hungary; [7]General and Adolescent Paediatric Unit, University College London, Institute of Child Health, London, UK; [8]Department of Infection, Immunity and Inflammation, Division of Child Health, University of Leicester, Leicester Royal Infirmary, Leicester, UK; [9]University of Szeged, Department of Pathology, Szeged, Hungary; [10]Department of Molecular and Clinical Genetics, Institute of Human Genetics, Polish Academy of Sciences, Poznan, Poland; [11]International Institute of Molecular and Cell Biology, Warsaw, Poland; [12]Department of Medical Genetics, University of Vienna, Vienna, Austria
*Correspondence: heymut.omran@uniklinik-freiburg.de
DOI 10.1016/j.ajhg.2008.10.001.

ODA defects.[9,10] Mutations in an ODA intermediate dynein chain, *DNAI1* (MIM 604366), are reported in 2%–13% of PCD patients with defined ODA defects.[11–13] Other genes that also encode ODA components, including *TXNDC3* and *DNAH11* (MIM 603339), only rarely account for PCD.[14–16] Here, we studied *DNAI2* (MIM 605483), the human ortholog of *Chlamydomonas* intermediate ODA chain *IC69/IC2* comprising 14 exons extending over 39 kb genomic distance.[17–19]

Applying a combinatory approach comprising positional and functional candidate-gene analyses, we identified three distinct recessive loss-of-function *DNAI2* mutations in six affected patients originating from three PCD families. In addition, we analyzed the role of DNAI2 in the assembly of ODA complexes by using transmission electron microscopy and high-resolution immunofluorescence imaging, which showed that DNAI2 is essential for ODA assembly throughout the ciliary axoneme.

Material and Methods

Patients and Families

We obtained signed and informed consent from patients who fulfilled diagnostic criteria of PCD[20] and from family members according to protocols approved by the Institutional Ethics Review Board at the University of Freiburg and collaborating institutions. We studied DNA from consanguineous kindred by total genome scan and mutational analysis. In addition, we sequenced all *DNAI2* exons from 105 PCD patients originating from unrelated families. The 105 affected individuals (56 females; 49 males) we analyzed are all white (age median 15 years, range from 2 years to 68 years), except for one affected Asian individual. In this cohort, 62 individuals had situs inversus (Kartagener Syndrome) and 43 situs solitus. Of the screened patients, 48 had ODA defects.

Linkage Analysis

A genome-wide linkage scan was carried out at the Wellcome Trust Centre for Human Genetics, Oxford, with the Illumina Linkage IV Panel of 6008 SNPs. In each sample, 98%–99% of the SNPs were successfully typed. Multipoint linkage analysis was performed with GeneHunter version 2.1r5, with the assumptions of autosomal-recessive inheritance, a disease allele frequency of 0.007, and complete penetrance. DNA samples from the family UCL149 and UCL150 parents and from affected (in total $n = 8$) but not unaffected offspring were typed in this scan.

Mutational Analysis

Genomic DNA was isolated by standard methods directly from blood samples or from lymphocyte cultures after Epstein-Barr virus transformation. Amplification of 14 genomic fragments comprising all 14 exons of *DNAI2* was performed in a volume of 50 μl containing 30 ng DNA, 50 pmol of each primer, 2 mM dNTPs, and 1.5 U *Taq* DNA polymerase (Eppendorf, Hamburg, Germany). PCR amplifications were carried out by means of an initial denaturation step at 94°C for 4 min and 33 cycles as follows: 94°C for 30 s, 53°C–64°C for 30 s, and 72°C for 60 s., with a final extension at 72°C for 10 min. PCR products were verified by agarose gel electrophoresis, column purified (Genomed, Loehne, Germany), and sequenced bidirectionally with BigDye Terminator v3.1 Cycle Sequencing Kit (Perkin Elmer). Samples were separated and analyzed on an Applied Biosystems 3730xl DNA Analyzer. Sequence data were evaluated with the Codoncode software (CodonCode Corporation, Dedham, MA. USA). To aid identification of frequent polymorphisms, we sequenced DNA of 13 healthy white controls (26 control chromosomes). In the families in which the affected individual carried the novel *DNAI2* mutations, other family members were also analyzed. We screened an additional 236 control chromosomes originating from healthy white individuals for the presence of the novel *DNAI2* mutation. Segregation analyses and screening of controls were performed by restriction analysis with MaeI (the MaeI restriction site is abrogated in affected individuals) and/or sequencing.

cDNA Analysis of Splicing Mutations

Total RNA was isolated from EBV-transformed lymphocytes from patients OP42-II2, UCL150Pa, and controls with trizol. First-strand cDNA synthesis was performed with the RevertAid H minus First Strand cDNA Synthesis Kit (Fermentas) and specific primers.

UCL150Pa: First-strand synthesis was performed with primer Ex12/13 (5′-ACT TGG TTG CTG AGG CAC TG-3′). The first PCR product was amplified with primers Ex9/10F (5′-TCC ATC ATG TGG ACC AAG TAC C-3′) and Ex12R1 (5′-TTA TGG CGT CTG CCT CCT TC-3′). Nested PCR with primers Ex10F (5′-GAG GCC GAC CGT TTT CTT TAC-3′) and Ex12R2 (5′-GCT CTG CGA AGA TGA TGT CG-3′) resulted in a wild-type product (425 bp) and a smaller product in patient UCL150Pa (278 bp). The PCR products were purified and sequenced bidirectionaly.

OP42-II2: The first-strand primer spans the junction of exons 6 and 7 (5′-GTC CCA GCA GGC TAT CTG TC-3′). The cDNA fragment comprising exons 3 and 5 was amplified with primers spanning the junction of exons 2 and 3 (Ex2/3F: 5′-GAA CAC GAG GCC AAC TCA G-3′) and exon 5 (Ex5R: 5′-GCT GAA AAT CCA AGC AGG AG-3′). Half-nested PCR with primers Ex3F (5′-GGG GAG TTA ACC ATG TCG AG-3′) and Ex5R showed a wild-type allele (351 bp) and in patient OP42-II2 a single-variant allele (229 bp). PCR products were gel purified and sequenced bidirectionally.

Immunoblotting

Protein extracts were prepared from human respiratory epithelial cell cultures according to previously published procedures.[20,28] Proteins were separated on a NuPAGE 4%–12% bis-tris gel (Invitrogen, Karlsruhe, Germany) and blotted onto a PVDF membrane (Amersham). The blot was processed for ECL plus (Amersham) detection with DNAI2 (1:1000) and anti-mouse-HRP (1:5000) antibodies (Santa Cruz, Heidelberg, Germany).

Immunofluorescence Analysis

Respiratory epithelial cells were obtained by nasal-brush biopsy (cytobrush plus, Medscand Malmö, Sweden) and suspended in cell-culture medium. Sperm cells were washed with phosphate-buffered saline. Samples were spread onto glass slides, air dried, and stored at −80°C until use. Cells were treated with 4% paraformaldehyde, 0.2% Triton X-100, and 1% skim milk prior to incubation with primary (at least 2 hr) and secondary (30 min) antibodies at room temperature. Appropriate controls were performed without the primary antibodies. Polyclonal rabbit DNAH5 and Dnali1 antibodies were described previously.[20,29] Mouse acetylated-α-tubulin antibodies were obtained from Sigma (Taufkirchen, Germany), and monoclonal mouse DNAI2 antibodies were obtained from Abnova Corporation (Taiwan). In addition, polyclonal

antibodies directed against DNAH9 were used. Highly cross-adsorbed secondary antibodies (Alexa Fluor 488, Alexa Fluor 546) were obtained from Molecular Probes (Invitrogen). DNA was stained with Hoechst 33342 (Sigma). Confocal images were taken on a Zeiss LSM 510 i-UV.

Transmission Electron Microscopy

The biopsies were taken from the middle turbinate. The sample of nasal mucosa was fixed in 2.5% glutaraldehyde in 0.1 M sodium cacodylate buffer at 4°C, washed overnight, and postfixed in 1% osmium tetroxide. After dehydration, the samples were embedded in a mixture of propylene oxide and epoxy resin. After polymerization, several resin sections were cut with an ultramicrotome. The sections were picked up onto copper grids. The sections were stained with Reynold's lead citrate. Transmission electron microscopy was performed with a Philips CM10.

Results

Positional and Functional Candidate-Gene Analyses Identified *DNAI2* Mutations

A total-genome linkage scan in a consanguineous Iranian Jewish kindred via single nucleotide polymorphisms (SNPs) detected only one genomic region (chromosome 17) with a significant LOD score ≥ 3. A 21.4 cM (9.6 Mb) region of homozygosity shared between the four affected offspring was identified on chromosome 17q25.1 across the *DNAI2* locus between flanking markers *rs755424* and *rs938350*; there was a maximum LOD score of 3.97 (Figure 1A) at marker *rs1872076*, which is located 780 kb centromeric to the start of *DNAI2*. Sequencing of all 14 *DNAI2* exons revealed a mutation, IVS11+1G > A, affecting the obligatory (100% sequence conservation) donor splice site of exon 11 (Figures 1B and 1C). Genotype analyses for this loss-of-function mutation showed cosegregation with the disease status in both nuclear families of the extended kindred (Figure 1B). Consistent with homozygosity by descent in the affected patients UCL149Pa, UCL149Pb, UCL150Pa, and UCL150Pb, the mutation was present in a homozygous state (Figures 1B and 1C, upper sequence). All parents (UCL149M and UCL149F, UCL150M, and UCL150F, Figure 1B) and one of the unaffected offspring (UCL149Na, Figure 1B) are heterozygous carriers. The unaffected offspring UCL149Nb and UCL150Nb (Figure 1B) are homozygous carriers of the wild-type allele (Figure 1C, lower sequence). Analysis of mutant cDNA of the affected individual UCL150Pa confirmed that the obligatory splicing mutation causes in-frame skipping of exon 11 (Figure 1D, right sequence), which predicts the loss of 49 amino acids. The clinical findings of the affected patients include neonatal pneumonia, recurrent rhinitis and sinusitis, recurrent otitis media and hearing deficits, chronic cough, and bronchiectasis. Two affected individuals had normal *situs solitus* (UCL149Pb, UCL150Pb), and two exhibited situs inversus (UCL149Pa, UCL150Pa), consistent with randomization of left/right body asymmetry. Infertility was reported in one of the affected males.

Further sequencing of all 14 coding exons, including the exon/intron boundaries, in 105 affected individuals originating from unrelated PCD families, including seven Hungarian families, revealed two novel *DNAI2* mutations. In a single white Hungarian PCD patient, OP42-II2, a facultative splicing mutation, IVS3-3T > G, located within the evolutionarily conserved (~80% conservation) splice acceptor site of exon 4, was identified (Figure 2A), and the change was absent in 236 control chromosomes of white individuals. The mutation cosegregated with the disease status in family OP42 and was present in the affected individual in a homozygous state (Figure 2B). Previous sequencing of all coding *DNAH5* exons in OP42 was normal.[10] To confirm that the DNA variant that is located within the splice acceptor site of intron 3 does indeed result in aberrant splicing, we performed RT-PCR analysis. A cDNA fragment comprising exons 3 and 5 was amplified in two rounds of amplifications with a specific first-strand primer spanning the junction between the exons 6 and 7. The PCR product of the affected individual OP42-II2 was reduced in size (229 bp), demonstrating that the mutation results in abnormal splicing. No wild-type allele was amplified (data not shown). Sequencing of the PCR product confirmed the absence of exon 4 and out-of-frame fusion of exon 3 to exon 5 (Figure 2C, upper sequence). RT-PCR analysis in control RNA (Figure 2C, lower sequence) elicited only wild-type transcripts that contained exon 4 (351bp). We conclude that the mutant splice site is not recognized by the splicing machinery and that this results in skipping of exon 4, and we thus predict early premature termination of translation because of out-of-frame transcripts (p.I116GfsX54). Interestingly, the family history did not reveal any known consanguinity of the parents. However, because both parents originate from the same geographical region (village), a distant relationship of both parents is most likely responsible for the homozygous mutation. To test whether the IVS3-3T > G mutation is especially prevalent in east Europe, we screened 125 Polish PCD patients and did not find this sequence variant. The second mutation (c.787C > T) was detected in a single white German PCD patient, OP254-II1. This homozygous C > T transversion at position 787 of exon 7 is a nonsense mutation, which leads us to predict early termination of translation (p.R263X, Figure 2D). Analysis of parental DNA revealed that both parents are heterozygous carriers of the mutation. In the affected members of the PCD families OP42 and OP254, we only detected polymorphisms in the homozygous state (Table S1 in the Supplemental Data). This finding is consistent with a distant relationship of the parents and is suggestive of "homozygosity by descent." Overall, the frequency of *DNAI2* mutations among our cohort is 1.9% (2/105 patients) and among the PCD families with ODA defects is 4.2% (2/48 patients).

The clinical findings of both patients comprised chronic otitis media, recurrent bronchitis and pneumonia, bronchiectasis, and situs inversus, consistent with Kartagener syndrome.

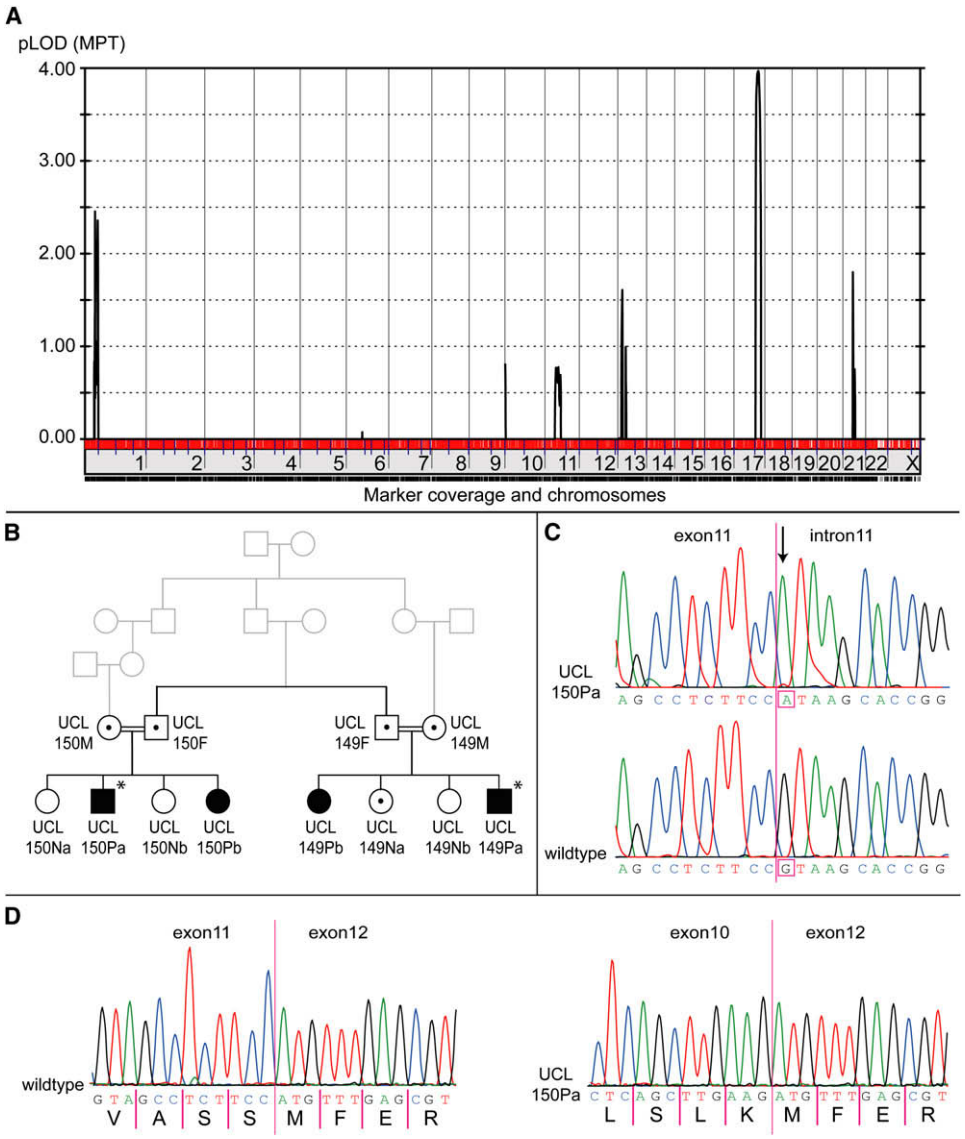

Figure 1. Linkage Scan and Homozygous Loss-of-Function *DNAI2* Mutations in a Large Consanguineous Kindred with Primary Ciliary Dyskinesia

(A) Multipoint linkage analysis performed with GeneHunter. A 21.4 cM (9.6 Mb) region of homozygosity shared between the affected offspring was identified on chromosome 17q25.1 across the *DNAI2* locus (maximum LOD score 3.97). Only the parents and affected children were used in the analysis.

(B) Pedigree of the consanguineous kindred with two related nuclear families. Affected children are represented by black symbols, and unaffected carriers are indicated by black dots. Asterisks indicate situs inversus.

(C) Sequence chromatographs of an affected patient (UCL150Pa, upper sequence) and a control individual (wt, lower sequence) showing the presence of the IVS11+1G > A mutation (black arrow). The detected loss-of-function mutation affects the obligatory splice donor site of exon 11 and is present in the homozygous state in all four affected children of the kindred. All parents (UCL149M and F, UCL150M and F) and one of the unaffected offspring (UCL149Na) are heterozygous carriers of the mutant allele. The unaffected offspring UCL149Nb and UCL150Nb are homozygous carriers for the wild-type allele.

(D) Results of cDNA analysis assessing the effect of the *DNAI2* splicing mutation IVS11+1G > A. In the mutant cDNA of the affected individual UCL150Pa (right sequence), the sequence of exon 11 is always absent. Thus, the splicing mutation leads to in-frame skipping of exon 11. Left sequence chromatograph depicts the cDNA sequence of a control subject.

Subcellular Localization of DNAI2 in Respiratory Cells and Sperm Cells

On the basis of its evolutionarily conserved homology to the *Chlamydomonas* intermediate ODA chain IC69/IC2 (44% identity[17,18]), we assumed that human DNAI2 plays a role in ODA assembly and function in cilia and flagella. Consistent with a function in cilia or flagella motility, *DNAI2* expression at the RNA level in respiratory cells and testis was reported previously.[18] To further corroborate that DNAI2 indeed functions specifically in ODA

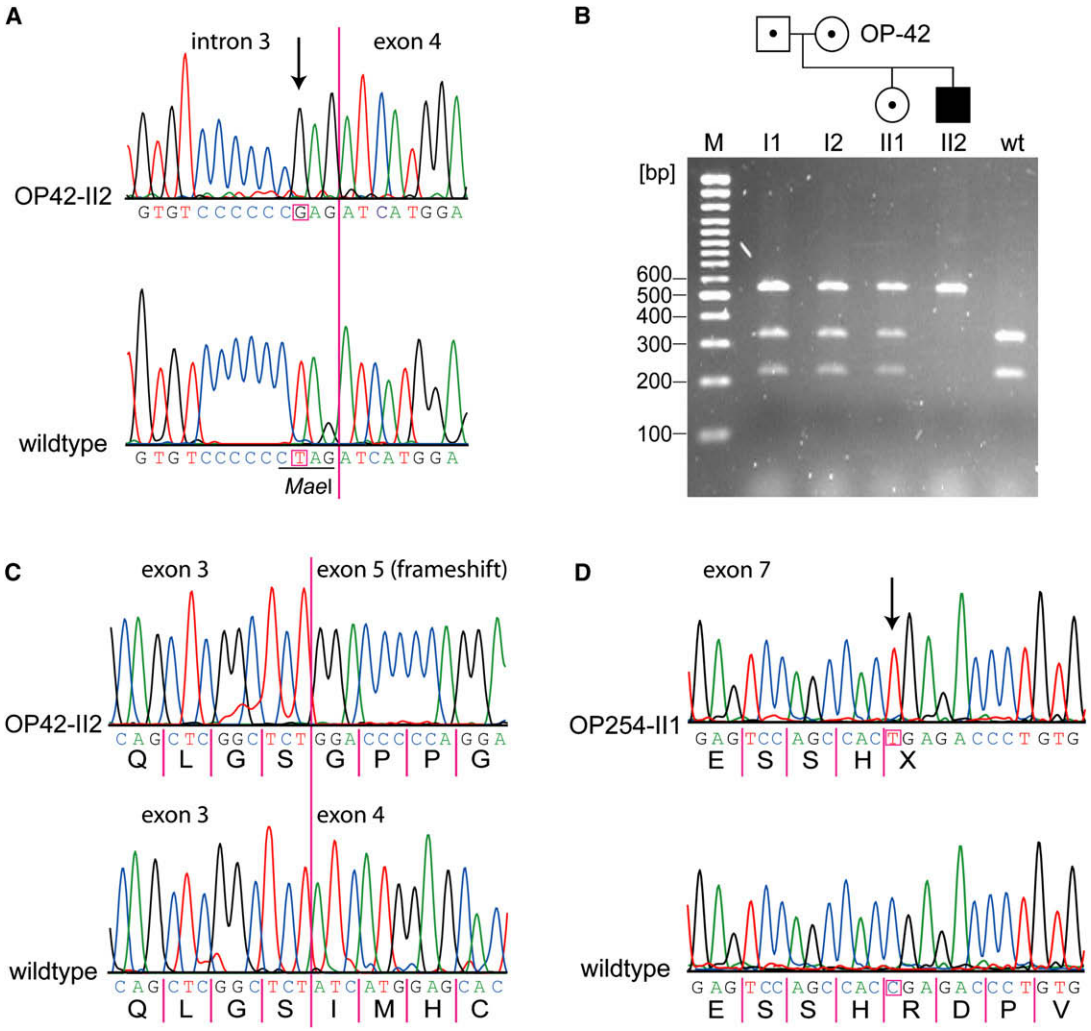

Figure 2. Recessive Loss-of-Function *DNAI2* Mutations in Patients with Primary Ciliary Dyskinesia

(A) A sequence chromatograph from the affected individual OP42-II2 shows a homozygous T > G transversion at position −3 of the exon 4 splice acceptor site (IVS3-3T > G; black arrow). For comparison, the wild-type sequence is shown. The mutation destroys a MaeI restriction site as indicated.

(B) Segregation analysis of the T > G transversion within the family. Presence of the mutation in the genomic DNA from all four family members was assessed by MaeI digestion of PCR products. The affected child (II2) showed a single (536 bp) band consistent with the presence of two mutant alleles abolishing the restriction sites in all PCR-amplified products. In contrast, in the control subject (wt), all PCR products are completely digested (324 bp and 212 bp bands). Restriction analyses in the unaffected sibling (II1), the mother (I2), and the father (I1) are consistent with heterozygous carrier status.

(C) Results of cDNA analysis assessing the effect of the *DNAI2* splicing mutation IVS3-3T > G. The lower sequence chromatograph depicts the cDNA sequence of a control subject. In the mutant cDNA of the affected individual OP42-II2 (upper sequence), the sequence of exon 4 is absent. Thus, the splicing mutation causes skipping of exon 4 and a frame shift that results in a premature stop codon (I116GfsX54).

(D) A genomic sequence chromatograph from the affected individual OP254-II1 shows a homozygous C > T transversion at position 787 of exon 7 (c.787C > T), predicting a premature stop codon and termination of translation (p.R263X, black arrow). For comparison, the wild-type sequence is shown.

complexes within respiratory cilia and sperm tails, we performed protein expression analyses with monoclonal antibodies directed against DNAI2. To confirm antibody specificity, we first performed immunoblot analyses of protein extracts from human respiratory cell cultures. DNAI2 antibodies detected a single band of ~69 kD, which corresponds to the predicted molecular weight of DNAI2 (Figure 3A). We next analyzed the subcellular localization of DNAI2 in human respiratory and sperm cells by using high-resolution immunofluorescence imaging. As a control, we used antibodies against the ODA heavy chain DNAH5. DNAI2 staining was observed throughout all analyzed respiratory ciliary axonemes and sperm flagella (Figures 3B and 3C), indicating that assembled ODA complexes along the entire length of these axonemes contain DNAI2.

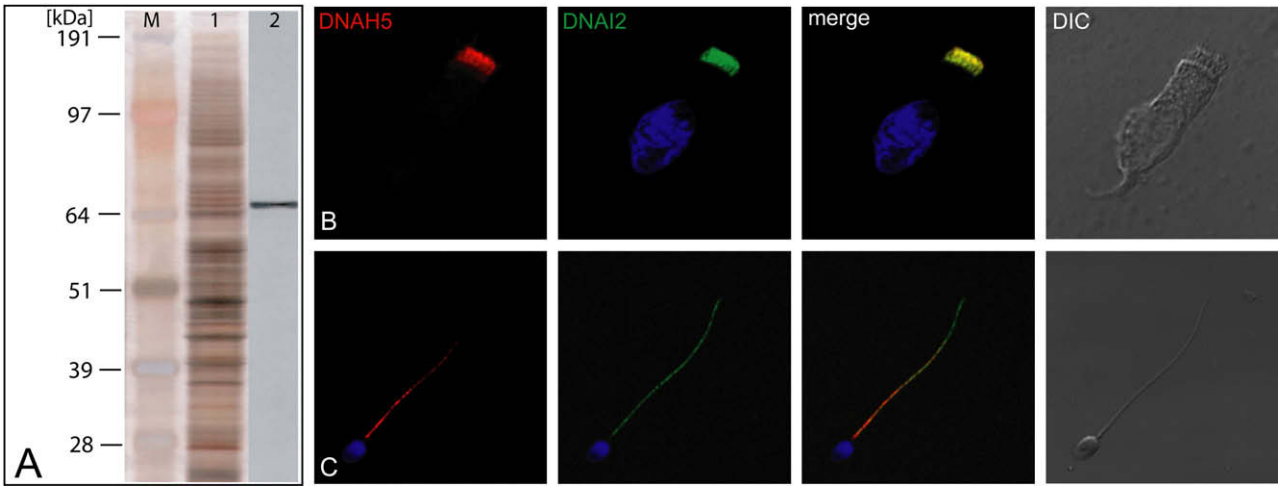

Figure 3. Specific Antibodies Localize the Human Axonemal Outer Dynein Arm Intermediate Chain 2 (DNAI2) to the Respiratory Ciliary Axoneme and Sperm Tail

(A) Western blot analysis of protein extracts from human nasal cell culture (M, protein standard; lane 1, silver staining). DNAI2 antibodies specifically detect a single band with the predicted size (~69 kD, lane 2).

(B and C) Immunofluorescence staining of human respiratory epithelial cells (B) and spermatozoa (C) with DNAI2 antibodies (green). DNAI2 is localized throughout all analyzed respiratory ciliary axonemes and sperm flagella. Ciliary axonemes and antibodies directed against axonemal outer sperm flagella were costained with dynein arm heavy chain DNAH5 (red). Note that DNAH5 also localizes throughout all respiratory ciliary axonemes but is only present in proximal sperm flagella, as reported previously.[20] Overlay and brightfield images are shown on the right side. Nuclei were stained with Hoechst 33342 (blue).

Characterization of ODA Defects Caused by the *DNAI2* Mutations

Next, we analyzed protein expression of *DNAI2* in respiratory cells that were obtained by nasal-brushing biopsy from patients UCL150Pa, OP42-II2, and OP254-II1, who harbor *DNAI2* mutations. Consistent with loss-of-function mutations, all analyzed cells lacked *DNAI2* expression (Figure 4), confirming the pathogenic significance of the detected mutations. As a control, we stained cilia with an antibody directed against the inner dynein arm light chain Dnali1, which is not altered by an ODA defect and can be used similarly to acetylated α-tubulin, to stain the axoneme. We have previously shown that respiratory cilia contain at least two distinct ODA types: type 1,DNAH9 negative and DNAH5 positive (proximal ciliary axoneme); type 2: DNAH9 and DNAH5 positive (distal ciliary axoneme).[20] High-resolution immunofluorescence imaging to detect the ODA heavy dynein chains DNAH5 and DNAH9 in respiratory cells from patients UCL150Pa, OP42-II2, and OP254-II1 showed an aberrant expression pattern for DNAH5 and DNAH9. DNAH5 protein was absent or severely reduced (Figure 5), and DNAH9 protein was undetectable in the ciliary axonemes of these PCD patients (Figure 6). Thus, we conclude that absence of DNAI2 prevents correct assembly of both ODA complexes (type 1 and type 2) in respiratory cells from patients UCL150Pa, OP42-II2, and OP254-II1; such a finding has so far only been reported for *DNAH5* mutations.[20] Consistent with these results, transmission electron microscopy of cross-sections of respiratory cilia from the patient UCL150Pb, who carries the IVS11+1G > A *DNAI2* mutation, detected ODA defects in all observed cross-sections at the ultrastructural level (Figure 5F). As expected, similar ultrastructural ODA defects were observed in transmission electron microscopy of respiratory cilia from patient OP42-II2 (Figure 5G).

Aberrant DNAI2 Localization in Respiratory Cells Harboring Mutations in *DNAH5*- and *DNAI1*-Encoding ODA Components

After the demonstration that DNAI2 deficiency can result in the complete absence of DNAH5 from respiratory ciliary axonemes, we investigated the effect of *DNAH5* mutations on DNAI2 expression. For this purpose we used respiratory cells from PCD patients carrying *DNAH5* mutations known to result in complete absence of DNAH5 from respiratory ciliary axonemes, as reported previously.[20] In respiratory cells from patient F661, who carries compound heterozygous *DNAH5* mutations 4361G > A (exon 28) and 8910+8911 delAT > insG (exon 53), we found complete absence of DNAI2 from all analyzed respiratory ciliary axonemes (Figure 7B). We further corroborated this finding in several other respiratory cells originating from various PCD patients with loss-of-function *DNAH5* mutations[10,20] (data not shown). Our findings indicate that DNAH5 is essential for correct assembly of DNAI2 in both types of ODA complexes.

Previously, we demonstrated that in respiratory cells of patients carrying homozygous *DNAI1* mutations IVS1+2_3insT, assembly of proximal ODA complexes (type 2) in the proximal ciliary axoneme is at least partially preserved: We found some residual localization of DNAH5

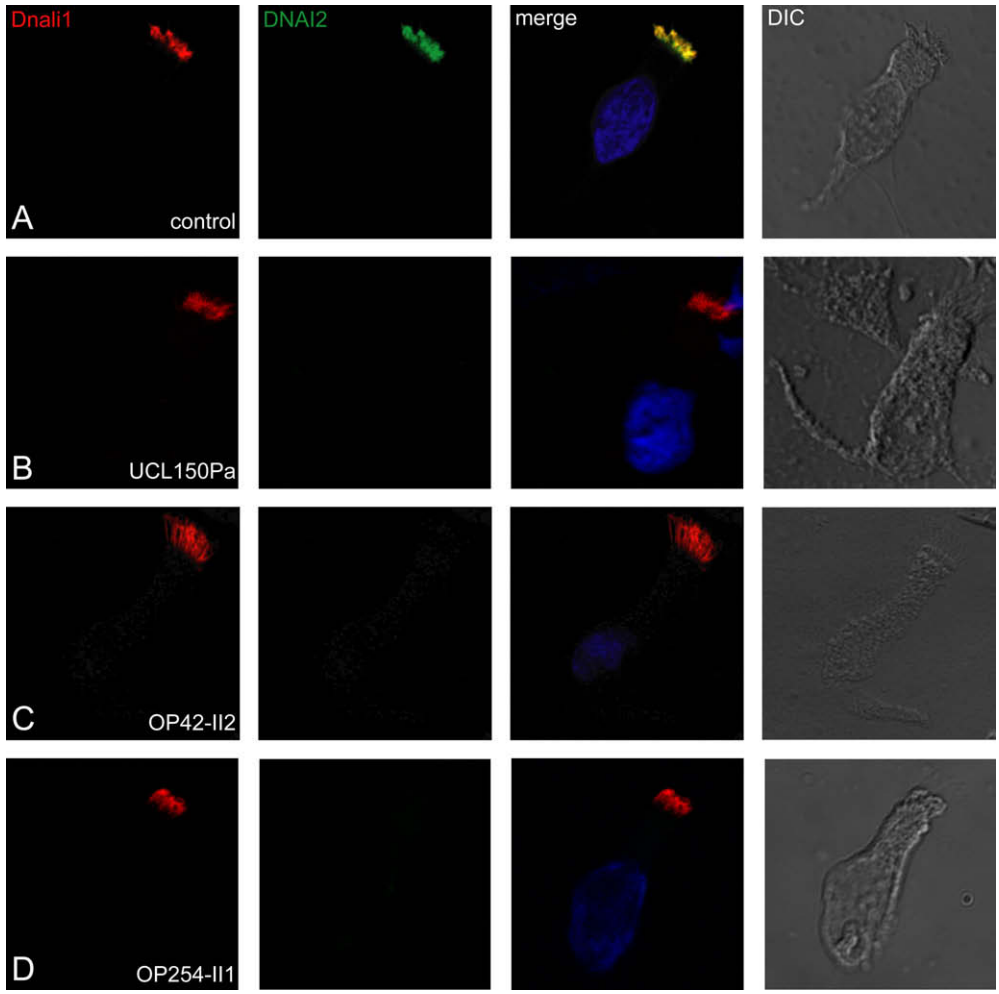

Figure 4. Absence of DNAI2 in Respiratory Epithelial Cells from Patients with Primary Ciliary Dyskinesia
Images of respiratory epithelial cells from a healthy control (A) and from patients carrying *DNAI2* mutations (B–D). Cells were costained with antibodies directed against outer dynein arm intermediate chain DNAI2 (green) and the inner-dynein-arm component Dnali1 (red) as control staining. Nuclei were stained with Hoechst 33342 (blue). (A) In control cells, DNAI2 localizes along the entire length of the respiratory ciliary axonemes. The yellow costaining within the ciliary axoneme indicates that both proteins colocalize within respiratory cilia. In cells of patient UCL150Pa (B), OP42-II2 (C) and OP254-II1 (D) DNAI2 is not detectable, consistent with recessive loss-of-function mutations that result in the failure to produce a functional DNAI2 protein.

in this proximal ciliary compartment, whereas DNAH5 was absent from the distal ciliary axoneme.[16] To investigate whether DNAI2 shows a similar localization pattern as DNAH5 in *DNAI1* mutant respiratory cells, we analyzed respiratory epithelial cells from patient OP121-II1, who carries the homozygous IVS1+2_3insT *DNAI1* mutation. Consistent with our previous finding that in *DNAI1* mutant cells assembly of proximal (type 2) ODA complexes is at least partially preserved, we found that DNAI2 staining was moderate in the proximal part but absent in the distal part of the ciliary compartment in all analyzed respiratory cells (Figure 7C).

Discussion

Outer dynein arm complexes are large multimeric protein complexes comprising light, intermediate, and heavy dynein chains, which are responsible for the generation of the cilia beat.[21] Recessive mutations of genes encoding the outer dynein arm components *DNAH5*, *DNAI1*, *TXNDC3*, and *DNAH11* can cause primary ciliary dyskinesia.[9–12,14–16] On the basis of this observation, we considered the outer dynein arm intermediate-chain gene *DNAI2* to be a functional candidate for primary ciliary dyskinesia. Here, we have identified the first PCD-causing *DNAI2* mutations affecting ODA assembly. The identified mutations most likely abrogate *DNAI2* function because premature stop codons (OP42-II2; OP254-II1) regularly result in nonsense-mediated RNA decay.[22] The IVS11+1G > A mutation detected in affected individuals of UCL149/150 (Figure 1C) predicts in-frame absence of 49 amino acids encoded by exon 11. Probably this truncated protein cannot function properly. Consistent with loss-of-function mutations, high-resolution immunofluorescence analysis revealed

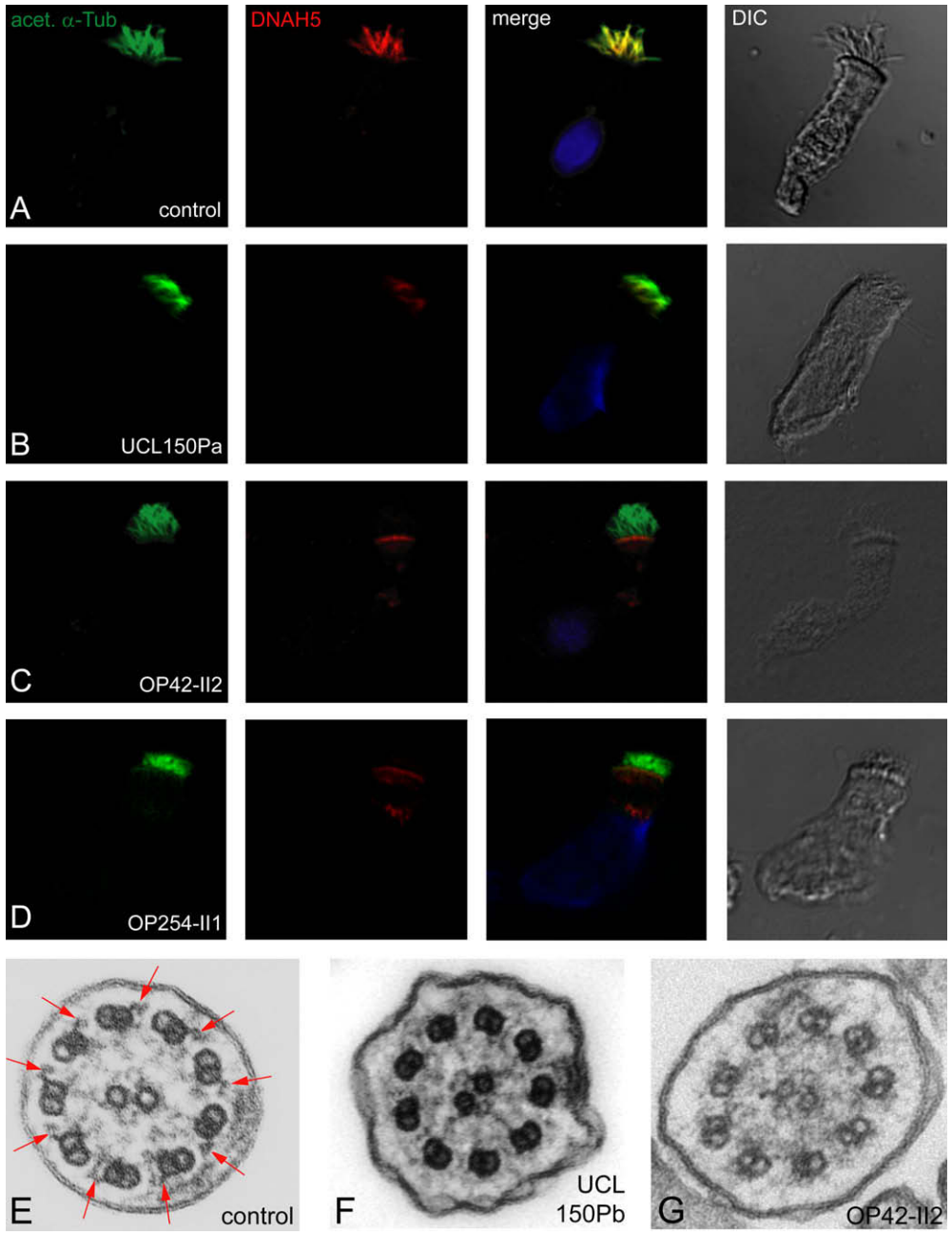

Figure 5. Mislocalization of the Outer Dynein Arm Heavy-Chain Protein DNAH5 in Respiratory Epithelial Cells from Patients with *DNAI2* Mutations

Images of respiratory epithelial cells from a healthy control (A) and from the patients UCL150Pa (B), OP42-II2 (C), and OP254-II1 (D) carrying the *DNAI2* mutations (B). Cells were costained with antibodies against acetylated α-tubulin (green) and DNAH5 (red). Nuclei were stained with Hoechst 33342 (blue). (A) In a healthy control, DNAH5 localizes along the entire length of the axonemes. The yellow color within the ciliary axoneme indicates that both proteins colocalize to cilia. (B, C, and D) In *DNAI2* mutant cells, DNAH5 is absent from the ciliary axonemes. (E, F, and G) Transmission electron micrographs of cross-sections from respiratory cilia originating from a healthy control (E) and from the DNAI2 patients UCL150Pb (F) and OP42-II2 (G). In the healthy control, outer dynein arms are visible ([E], red arrows), whereas in the patients UCL150Pb (F) and OP42-II2 (G), they are absent.

that affected individuals of all three analyzed families lacked any detectable DNAI2 protein expression in respiratory cells (Figure 4).

The *DNAI2* mutations identified appear to result in randomization of left/right body asymmetry: Of the six affected individuals carrying *DNAI2* mutations, two exhibited situs solitus, and four exhibited situs inversus. All affected individuals suffered from chronic lung disease. Infertility in one male was reported, but no sperm analysis was available. Consistent with the observed clinical phenotype of this PCD subtype, comprising lack of appropriate airway clearance by respiratory cilia and male

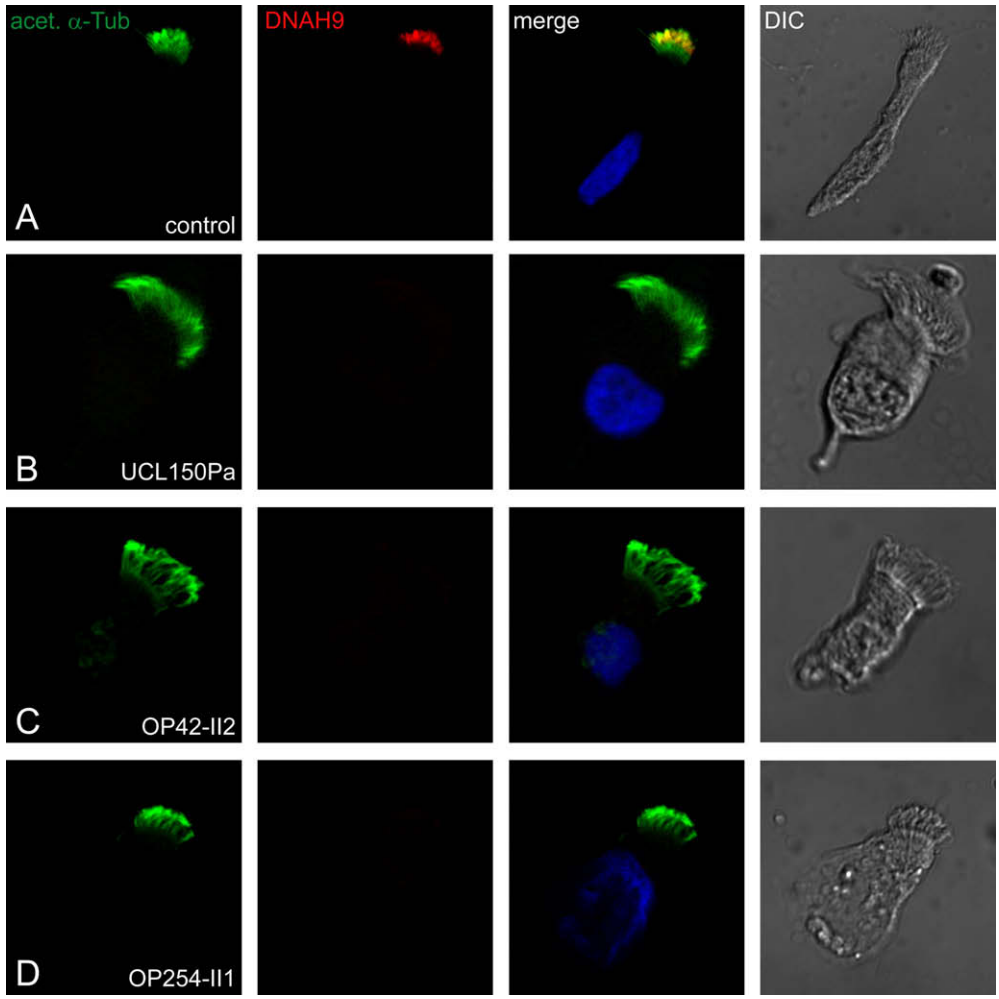

Figure 6. Absence of the Outer Dynein Arm Heavy-Chain Protein DNAH9 in Respiratory Epithelial Cells from Patients with *DNAI2* Mutations

Images of respiratory epithelial cells from a healthy control (A) and from patients UCL150Pa (B), OP42-II2 (C), and OP254-II1 (D), who carry *DNAI2* mutations. Cells were co-stained with antibodies against acetylated α-tubulin (green) and DNAH9 (red). Nuclei were stained with Hoechst 33342 (blue). (A) In control cells DNAH9 localizes in the distal part of the respiratory ciliary axonemes. The yellow co-staining within the ciliary axoneme indicates that both proteins co-localize within respiratory cilia. In respiratory cells of patient UCL150Pa (B), OP42-II2 (C) and OP254-II1 (D) DNAH9 is not detectable in the ciliary axonemes.

infertility, we detected DNAI2 protein expression in respiratory cilia and sperm flagella (Figure 3). The randomization of left/right body asymmetry is probably explained by an altered motility of nodal cilia responsible for determination of left/right body asymmetry.[5]

We have previously shown that, in contrast to those in *Chlamydomonas,* human ODA complexes vary in their composition along the respiratory ciliary axoneme and the axoneme of the sperm tail and that this composition also differs between these two cell types.[20] Respiratory cilia contain at least two distinct ODA types: type 1, DNAH9 negative and DNAH5 positive (proximal ciliary axoneme); and type 2, DNAH9 and DNAH5 positive (distal ciliary axoneme). To determine the subcellular localization of DNAI2 in various cell types carrying motile cilia or flagella, we used specific monoclonal mouse antibodies directed against human DNAI2 for high-resolution immunofluorescence microscopy (Figure 3A). We demonstrated localization of DNAI2 throughout the entire length of axonemes from respiratory cilia as well as sperm tails (Figures 3B and 3C). This finding indicates that DNAI2 is present in both ODA (type 1 and 2) complexes.

Interestingly, mutations of the distinct genes encoding ODA components do not result in identical defects. We have shown that *DNAH5* and *DNAI1* mutations regularly result in absent and/or shortened ODAs visualized by transmission electron microscopy.[9,10,12,23,24] In contrast the *DNAH11* mutations reported so far do not result in ultrastructural defects detectable by routine transmission-electron microscopy,[14,16] and *TXNDC3* mutant cilia exhibit both normal and abnormal cilia cross-sections.[15] To determine the effect of *DNAI2* mutations on axonemal ultrastructure, we performed transmission electron microscopy. Cilia cross-sections showed ODA defects (Figures 5F

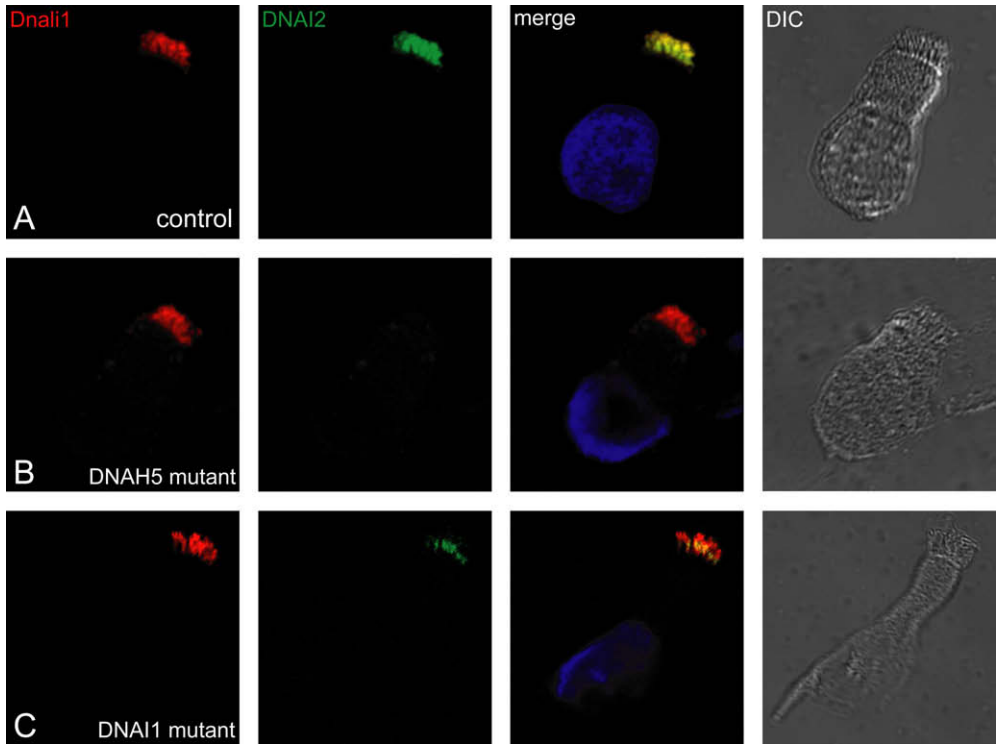

Figure 7. Mis-localization of outer dynein arm chain DNAI2 in respiratory epithelial cells from PCD patients carrying mutations in the outer dynein arm components *DNAH5* and *DNAI1*

Images of respiratory epithelial cells from healthy control (A), compound heterozygote patient carrying the *DNAH5* mutations 4361G > A (exon 28) and 8910+8911 delAT > insG (exon 53) (B) and a patient homozygous for the *DNAI1* mutation IVS1+2_3insT (C). Cells are costained with antibodies directed against DNAI2 (green) and against inner dynein arm component Dnali1 as a control (red). Nuclei were stained with Hoechst 33342 (blue). In *DNAH5* mutant cells (B), DNAI2 is absent from the ciliary axonemes, indicating that DNAH5 is necessary for DNAI2 assembly. In *DNAI1* mutant cells (C), DNAI2 (green) is absent from the distal part of the axonemes but is still detectable in the proximal ciliary axoneme. This indicates that mutant DNAI1 inhibits assembly of DNAI2 predominantly in the distal ciliary axonemes.

and 5G) resembling defects identified in patients with *DNAH5* mutations.[9] To analyze this further, we performed high-resolution immunofluorescence analysis in respiratory cilia from patients UCL150Pa, OP42-II2, and OP254-II1, who had *DNAI2* mutations. Consistent with deficient assembly of ODA types 1 and 2, we found absence or severe reduction of the ODA heavy chains DNAH5 and DNAH9 from the entire ciliary axoneme (Figures 5 and 6). Our findings indicate that DNAI2 is essential for axonemal assembly of the ODA heavy chains DNAH5 and DNAH9 in the analyzed respiratory cells of patients UCL150Pa, OP42-II2, and OP254-II1. This observation resembles findings reported in respiratory cilia of patients carrying *DNAH5* loss-of-function mutations.[10,20] Therefore, we also analyzed respiratory cilia from patients with *DNAH5* mutations for DNAI2 expression. DNAI2 expression within the analyzed respiratory cilia was completely absent (Figure 7B), demonstrating in a complementary manner that DNAH5 is also essential for the axonemal assembly of the ODA protein DNAI2 within ODA types 1 and 2.

Furthermore, we analyzed respiratory cilia from a patient carrying a homozygous *DNAI1* mutation for DNAI2 localization. DNAI2 expression was restricted to the proximal part of the respiratory cilia and was completely missing in the distal part of the ciliary axoneme (Figure 7C). We previously reported a similar staining pattern for DNAH5 in DNAI1 mutant cells.[16] These findings indicate that mutant DNAI1 in these cells predominantly inhibits axonemal assembly of distally localized ODA types, whereas proximal ODAs can at least become partially assembled.

Previous findings in *Chlamydomonas reinhardtii* support an evolutionarily conserved functional role for DNAI2 in ODA assembly; this role is similar to that shown here in the human axoneme. Fowkes and Mitchell[25] analyzed the stability of ODA complexes in the cytoplasm of wild-type *Chlamydomonas* and several outer dynein-arm mutant strains. Interestingly, in the *Chlamydomonas oda6* mutant carrying mutations of the *IC69/IC2* gene, which is orthologous to *DNAI2*,[26] the ODA complexes were disrupted, indicating the importance of DNAI2/IC69/IC2 for ODA assembly. In addition, a similar phenotype was observed in the *pf28/oda2* mutant carrying a mutation in the γ-dynein heavy chain orthologous to *DNAH5*,[27] which is also consistent with our findings of an absence of DNAI2 assembly in DNAH5 mutant cells (Figure 7B).

Interestingly, our data also show that *DNAI1* mutations do not necessarily inhibit ODA assembly of proximal ODA complexes, indicating that evolution has given DNAI1 functional roles not played by DNAI2 because mutations of the *Chlamydomonas* orthologs IC1 and IC2 exhibit identical findings.[27] Thus, DNAI1 might have obtained similar functions to those of TXNDC3 because *TXNDC3* mutant cilia exhibit both normal and abnormal cilia cross-sections, suggesting that it also mainly affects one of the two distinct ODA complexes.[15] However, so far it is not known for which type of ODA complex (distal or proximal) TXNDC3 plays an important functional role.

Our findings that mutations in *DNAI2* cause PCD due to ODA defects enhance our understanding of the molecular basis of this chronic respiratory disease and support previous data that humans have at least two distinct ODA complexes. Early diagnosis of PCD is important for appropriate health management with the goal of preventing or delaying lung damage.[3] The use of DNAI2 antibodies can augment antibody-based PCD diagnostic techniques, such as immunofluorescence analyses. The demonstration of *DNAI2* mutations will aid development of genetic screening for PCD and enable appropriate genetic counseling in affected individuals. Further mutational analyses will clarify whether, like *DNAH5* mutations, *DNAI2* mutations can also account for heterotaxia with severe congenital heart defects.[6]

Supplemental Data

Supplemental Data include one table and are available with this article online at http://www.ajhg.org/.

Acknowledgments

We are grateful to the patients and their families for their participation in this study. We thank the German patient support group Kartagener Syndrom und Primaere Ciliaere Dyskinesie e.V. We thank R. Nitschke and S. Haxelmans at the life imaging center, Institute for Biology I, University Freiburg, for their excellent support with confocal microscopy. We thank C. Reinhard, A. Heer, A. Schwentek, E. Rutkiewicz, and K. Parker for excellent technical assistance. We would also like to thank Andrzej Pogorzelski from the Institute of Tuberculosis and Lung Diseases, Rabka for clinical diagnosis and recruitment of patients. This work was supported by Deutsche Forschungsgemeinschaft grants DFG Om 6/4, GRK1104, and SFB592 (to H.O.), and by grants from the Polish State Committee for Scientific research (PBZ KBN 122/P05-1, to E.Z.), the National Specialist Commissioning Advisory Group, UK (to C.O'C.), and the Milena Carvajal–Prokartagener Foundation (to H.M.M.). This work is dedicated to Bjorn A. Afzelius for his outstanding research in the field of ciliary structure and immotile-cilia syndrome.

Received: August 8, 2008
Revised: September 19, 2008
Accepted: October 1, 2008
Published online: October 23, 2008

Web Resources

URLs for data presented herein are as follows:

Online Mendelian Inheritance in Man (OMIM), http://www.ncbi.nlm.nih.gov/Omim/
dbSNP NCBI database, http://www.ncbi.nlm.nih.gov/SNP/
ENSEMBL, http://www.ensembl.org/index.html

References

1. Afzelius, B.A. (1976). A human syndrome caused by immotile cilia. Science *193*, 317–319.
2. Fliegauf, M., Benzing, T., and Omran, H. (2007). When cilia go bad: Cilia defects and ciliopathies. Nat. Rev. Mol. Cell Biol. *8*, 880–893.
3. Meeks, M., and Bush, A. (2000). Primary ciliary dyskinesia (PCD). Pediatr. Pulmonol. *29*, 307–316.
4. Geremek, M., and Witt, M. (2004). Primary ciliary dyskinesia: Genes, candidate genes and chromosomal regions. J. Appl. Genet. *45*, 347–361.
5. Nonaka, S., Tanaka, Y., Okada, Y., Takeda, S., Harada, A., Kanai, Y., Kido, M., and Hirokawa, N. (1998). Randomization of left-right asymmetry due to loss of nodal cilia generating leftward flow of extraembryonic fluid in mice lacking KIF3B motor protein. Cell *95*, 829–837.
6. Kennedy, M.P., Omran, H., Leigh, M.W., Dell, S., Morgan, L., Molina, P.L., Robinson, B.V., Minnix, S.L., Olbrich, H., Severin, T., et al. (2007). Congenital heart disease and other heterotaxic defects in a large cohort of patients with primary ciliary dyskinesia. Circulation *115*, 2814–2821.
7. Zariwala, M.A., Knowles, M.R., and Omran, H. (2007). Genetic defects in ciliary structure and function. Annu. Rev. Physiol. *69*, 423–450.
8. Pazour, G.J., Agrin, N., Walker, B.L., and Witman, G.B. (2006). Identification of predicted human outer dynein arm genes: candidates for primary ciliary dyskinesia genes. J. Med. Genet. *43*, 62–73.
9. Olbrich, H., Haffner, K., Kispert, A., Volkel, A., Volz, A., Sasmaz, G., Reinhardt, R., Hennig, S., Lehrach, H., Konietzko, N., et al. (2002). Mutations in *DNAH5* cause primary ciliary dyskinesia and randomization of left-right asymmetry. Nat. Genet. *30*, 143–144.
10. Hornef, N., Olbrich, H., Horvath, J., Zariwala, M.A., Fliegauf, M., Loges, N.T., Wildhaber, J., Noone, P.G., Kennedy, M., Antonarakis, S.E., et al. (2006). *DNAH5* mutations are a common cause of primary ciliary dyskinesia with outer dynein arm defects. Am. J. Respir. Crit. Care Med. *15*, 120–126.
11. Pennarun, G., Escudier, E., Chapelin, C., Bridoux, A.M., Cacheux, V., Roger, G., Clement, A., Goossens, M., Amselem, S., and Duriez, B. (1999). Loss-of-function mutations in a human gene related to *Chlamydomonas reinhardtii* dynein IC78 result in primary ciliary dyskinesia. Am. J. Hum. Genet. *65*, 1508–1519.
12. Zariwala, M.A., Leigh, M.W., Ceppa, F., Kennedy, M.P., Noone, P.G., Carson, J.L., Hazucha, M.J., Lori, A., Horvath, J., Olbrich, H., et al. (2006). Mutations of *DNAI1* in primary ciliary dyskinesia: Evidence of founder effect in a common mutation. Am. J. Respir. Crit. Care Med. *15*, 858–866.
13. Failly, M., Saitta, A., Muñoz, A., Falconnet, E., Rossier, C., Santamaria, F., de Santi, M.M., Lazor, R., Delozier-Blanchet, C.D., Bartoloni, L., et al. (2008). DNAI1 mutations explain only 2% of primary ciliary dykinesia. Respiration *76*, 198–204. Published online April 23, 2008. 10.1159/000128567.

14. Bartoloni, L., Blouin, J.L., Pan, Y., Gehrig, C., Maiti, A.K., Scamuffa, N., Rossier, C., Jorissen, M., Armengot, M., Meeks, M., et al. (2002). Mutations in the *DNAH11* (axonemal heavy chain dynein type 11) gene cause one form of *situs inversus totalis* and most likely primary ciliary dyskinesia. Proc. Natl. Acad. Sci. USA *99*, 10282–10286.
15. Duriez, B., Duquesnoy, P., Escudier, E., Bridoux, A.M., Escalier, D., Rayet, I., Marcos, E., Vojtek, A.M., Bercher, J.F., and Amselem, S. (2007). A common variant in combination with a nonsense mutation in a member of the thioredoxin family causes primary ciliary dyskinesia. Proc. Natl. Acad. Sci. USA *104*, 3336–3341.
16. Schwabe, G.C., Hoffmann, K., Loges, N.T., Birker, D., Rossier, C., de Santi, M.M., Olbrich, H., Fliegauf, M., Failly, M., Liebers, U., et al. (2008). Primary ciliary dyskinesia associated with normal axoneme ultrastructure is caused by *DNAH11* mutations. Hum. Mutat. *29*, 289–298.
17. Pfister, K.K., Fay, R.B., and Witman, G.B. (1982). Purification and polypeptide composition of dynein ATPases from *Chlamydomonas* flagella. Cell Motil. *2*, 525–547.
18. Pennarun, G., Chapelin, C., Escudier, E., Bridoux, A.M., Dastot, F., Cacheux, V., Goossens, M., Amselem, S., and Duriez, B. (2000). The human dynein intermediate chain 2 gene (*DNAI2*): cloning, mapping, expression pattern, and evaluation as a candidate for primary ciliary dyskinesia. Hum. Genet. *107*, 642–649.
19. Lonergan, K.M., Chari, R., Deleeuw, R.J., Shadeo, A., Chi, B., Tsao, M.S., Jones, S., Marra, M., Ling, V., Ng, R., et al. (2006). Identification of novel lung genes in bronchial epithelium by serial analysis of gene expression. Am. J. Respir. Cell Mol. Biol. *35*, 651–661.
20. Fliegauf, M., Olbrich, H., Horvath, J., Wildhaber, J.H., Zariwala, M.A., Kennedy, M., Knowles, M.R., and Omran, H. (2005). Mislocalization of DNAH5 and DNAH9 in respiratory cells from patients with primary ciliary dyskinesia. Am. J. Respir. Crit. Care Med. *171*, 1343–1349.
21. Ibanez-Tallon, I., Heintz, N., and Omran, H. (2003). To beat or not to beat: Roles of cilia in development and disease. Hum. Mol. Genet. *1*, R27–R35.
22. Chang, Y.F., Imam, J.S., and Wilkinson, M.F. (2007). The nonsense-mediated decay RNA surveillance pathway. Annu. Rev. Biochem. *76*, 51–74.
23. Omran, H., Haffner, K., Volkel, A., Kuehr, J., Ketelsen, U.P., Ross, U.H., Konietzko, N., Wienker, T., Brandis, M., and Hildebrandt, F. (2000). Homozygosity mapping of a gene locus for primary ciliary dyskinesia on chromosome 5p and identification of the heavy dynein chain *DNAH5* as a candidate gene. Am. J. Respir. Cell Mol. Biol. *23*, 696–702.
24. Kispert, A., Olbrich, H., Volz, A., Ketelsen, U.P., Horvath, J., Melkaoui, R., Petry, M., Zariwala, M., Noone, P.G., Knowles, M., et al. (2003). Genotype-phenotype correlations in PCD patients carrying *DNAH5* mutations. Thorax *58*, 552–554.
25. Fowkes, M.E., and Mitchell, D.R. (1998). The role of preassembled cytoplasmic complexes in assembly of flagellar dynein subunits. Mol. Biol. Cell *9*, 2337–2347.
26. Mitchell, D.R., and Kang, Y. (1991). Identification of *oda6* as a *Chlamydomonas* dynein mutant by rescue with the wild-type gene. J. Cell Biol. *113*, 835–842.
27. Mitchell, D.R., and Rosenbaum, J.L. (1985). A motile *Chlamydomonas* flagellar mutant that lacks outer dynein arms. J. Cell Biol. *100*, 1228–1234.
28. Olbrich, H., Horvath, J., Fekete, A., Loges, N.T., van's Gravesande, K.S., Blum, A., Hormann, K., and Omran, H. (2006). Axonemal localization of the dynein component DNAH5 is not altered in secondary ciliary dyskinesia. Pediatr. Res. *59*, 418–422.
29. Rashid, S., Breckle, R., Hupe, M., Geisler, S., Doerwald, N., and Neesen, J. (2006). The murine *Dnali1* gene encodes a flagellar protein that interacts with the cytoplasmic dynein heavy chain 1. Mol. Reprod. Dev. *73*, 784–794.